Chapter 3
Automatic Glaucoma Diagnosis in Digital Fundus Images Using Deep CNNs

Ambika Sharma, Monika Agrawal, Sumantra Dutta Roy and Vivek Gupta

1 Introduction

Globally, eye diseases are increasing at an alarming rate. The top three eye diseases are cataract, glaucoma, and age-related macular degeneration (AMD). Talking about "glaucoma", which is the second leading cause of blindness in the world and number one blinding disease among African Americans, scientific evidences show that if early diagnosis and treatment are given during early stages, then permanent loss of vision can be prevented in at least 60% of the cases [1]. Thus, there is a pressing need to develop a cost-effective computer-based automatic diagnostic system that can assist medical experts in early diagnosis, thus save their time and efforts wasted on the analysis of healthy people. Glaucoma is a chronic eye disease in which the optic nerve gets gradually damaged and thus leads to permanent loss of vision [2, 3]. It is also called the "silent thief of sight" because the loss of sight usually occurs over a long period of time. Eye experts use specialized devices for the eye monitoring such as a slit lamp or an ophthalmoscope to look at the back of the eye. These ophthalmologists are able to evaluate the health of an eye by looking at the various

A. Sharma (✉)
Bharti School of Telecommunication Technology and Management (BSTTM), IITD, New Delhi, India
e-mail: Ambika.Sharma@dbst.iitd.ac.in

M. Agrawal
Centre for Applied, New Delhi, India
e-mail: Monika.Aggarwal@care.iitd.ac.in

S. D. Roy
Electrical Department, IITD, New Delhi, India
e-mail: sumantra@ee.iitd.ac.in

V. Gupta
AIIMS Delhi, New Delhi, India
e-mail: vgupta@aiims.edu

S. Jain et al. (eds.), *Advances in Computational Intelligence Techniques*, Algorithms for Intelligent Systems,
https://doi.org/10.1007/978-981-15-2620-6_3

characteristics of cup and disc such as colour, contour, and diameter and thus able to predict the presence of disease based on their experiences and knowledge. Usually, for the glaucoma diagnosis, the two main indicators are the cup-to-disc ratio (CDR) and inferior-superior-nasal-temporal (ISNT) area rule [4], and for the calculation of these parameters, it is necessary to segment the optic disc and cup simultaneously. Figures 1, 2, and 3 show some of the examples of healthy and glaucomatous retinal images from the database. Figure 2 clearly shows the glaucoma image with high cup-to-disc ratio, and Fig. 3 shows the inferior rim loss retinal image, respectively. As mentioned previously, glaucoma is frequently known as "the sneak thief of sight" because of gradual rise in intraocular pressure and damage of the optic nerve or vision. The disease shows no early symptoms in the majority of the cases [5]. Thus, it is important to raise awareness among mass public for early detection and regular examination of eyes as this is still successfully controllable at the early stage if treated properly.

A number of algorithms have already been proposed for the glaucoma detection [5–21]. Researchers have categorized the detection into two parts. In the first category, the diagnosis requires the complete optic disc and cup boundary knowledge for the cup-to-disc feature calculation and other experimentation's [7, 11, 13, 14, 22], whereas the other approach deals directly with the complete image and learns its own set of feature for final decision [15, 21]. The first approach includes various methods, and some of them are as follows. Wong et al. [23], citeb26 suggested level set method for disc extraction and a blood vessel kink detection along with variational level set-based method for cup segmentation. An ellipse is fitted to the obtained cup boundary so as to get an initial estimate based on pallor and to the disc boundary to get a regular shape of region of interests. The method used canny edge

Fig. 1 Healthy image

Fig. 2 High CDR (glaucoma)

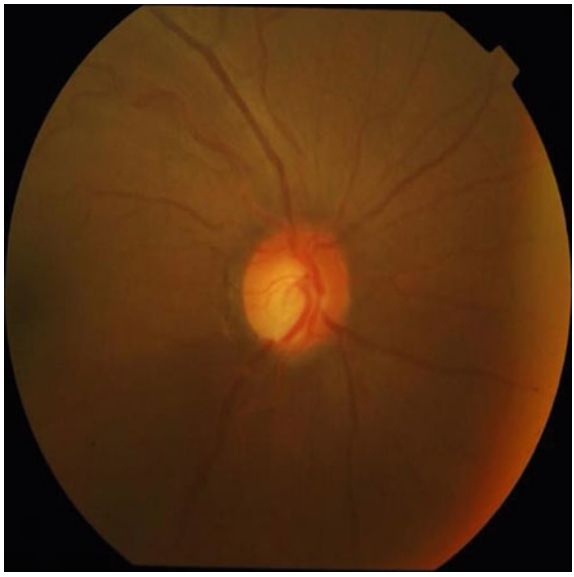

Fig. 3 Inferior rim loss (glaucoma)

detection along with the wavelet transform on the green channel image to detect the kinks on the intra-optic disc vessel edges. The extended work of this is mentioned in [24] which uses segmented disc and cup regions from level set approach to find the cup-to-disc Ratio (CDR) for glaucoma analysis. Cheng et al. [25] has also suggested

an efficient approach based on super-pixel classification. The algorithm uses a simple linear clustering algorithm to collect the nearby pixels into superpixels. A set of OD and OC features have been constructed using histogram equalization of all three components. A support vector machine (SVM)-based library was used to classify the pixels as disc or non-disc in the OD and for OC segmentation, respectively. Yin et al. [26] have introduced model-based method along with circular Hough transform (CHT) for detection. From the last few years tremendous amount of effort has been done in glaucoma detection using machine learning techniques. Support vector machine, K-nearest neighbour, regression models, neural network, fuzzy min–max neural network, decision tree-based algorithms are some of the key techniques to perform automatic detection of glaucoma. The work proposed in [27] uses CNNs to learn the hierarchical information of retinal image and performs the optic disc and cup segmentation. The approach uses two neural networks, one for disc segmentation followed by a deep neural network of cup segmentation. For glaucoma prediction, it uses radii ratio of cup over disc along with the square root of areas of cup over disc. Recently, a novel approach proposed by Chen [21] where the network has used four convolutional layers and two fully connected layers. The network inputs the cropped OD regions for training and testing of the network. The obtained AUC values are 0.831 and 0.887 for ORIGA and SCES datasets. Another novel work by [28] utilizes sliding window idea using deep learning for glaucoma diagnosis. The system uses a bundle of sliding windows of different sizes to obtain the cup regions in each disc image, cropped from complete retinal image. It then extracts the features corresponding to each cup candidate using histogram method learned using a group sparsity constraint. The approach uses support vector regression model to rank each candidate region, and final prediction is made using non-maximal suppression method. In glaucoma screening, cup extraction has been suggested to be the toughest task. Thus, [29] suggested an efficient reconstruction approach to localize cup region for glaucoma diagnosis. The method has a code-book of reference disc and cup images, and the problem of finding the coordinates and radius of cup has been modelled as an optimization problem with the sparsity constraint. The results have been validated on SCES and ORIGA dataset. One of the key contributions in glaucoma screening is provided by [30] which uses U-Net for optic disc and cup segmentation and the uses four ImageNet-pre-trained CNN networks to classify glaucoma disease. Further, [31] uses cup-to-disc ratio as the key indicator for glaucoma and thus utilizes segmentation algorithms to find the disc and cup boundaries. The paper starts with OD detection method using the template matching and brightness property of optic disc. Later, it uses this apriori knowledge of optic disc area to find the disc and cup boundaries using the texture-based and model-based approach. The method achieves 98% accuracy on final glaucoma screening and diagnosis for Drishti dataset. Mvoulana et al. [31] work has been based on deep convolutional neural networks to segment the optic disc and cup regions for glaucoma diagnosis. The network is motivated by the DenseNet architecture which uses *U*-shape network to perform the pixel-wise classification. Another important work in the field is proposed by [32], where the paper has done an extensive study of different convolutional network for glaucoma diagnosis purpose. The method has used all existing classification networks to validate

the retinal images as healthy or glaucoma. It has also incorporated the pre-trained weights of Imagenet dataset on existing architectures. Another approach has been suggested by [33] to diagnose glaucoma using deep convolutional neural network (CNN) unsupervised architecture which extracts the multilayer features from raw pixel intensities. Afterwards, the deep-belief network (DBN) model was used to select the most discriminative deep features based on the training dataset. At last, [34, 35] presents other work on glaucoma diagnosis using deep convolutional neural networks. Motivated by recent success in deep learning in biomedical image disease diagnosis, we have proposed a deep CNN architecture. As discussed, earlier CNN has wider applications in various domains right from face detection by Facebook, photo search by Google and recommendation models by Amazon.

The performance of all non-deep learning techniques depends upon the features being selected for classification. Also, in case of pathological conditions (presence of lesions, exudates, and light artifacts), it becomes difficult to precisely extract the suitable features for classification. Thus, it is important for a model to learn all the best possible features to extract, maximum possible information from the image, even in the presence of some other artifacts say light, or lens aberrations, thus avoids the need of hand-crafted features. The key idea behind our approach is to design an algorithm which incorporates both set of features, i.e. local and global, and enables us to predict the results with better accuracy. The obtained detection accuracy is 99.98% on the training and on tested dataset is 90.5%. The proposed algorithm has been discussed in following sections. Section 2 gives the brief introduction and motivation for proposed algorithm. In Sect. 3, some light has been shed on understanding the concept of deep neural networks. Later, Sect. 4 briefly introduces the proposed deep architecture for glaucoma diagnosis. At last, Sect. 5 shows the experimental and simulated results, followed by the conclusion in Sect. 6 for the proposed work.

2 Proposed Algorithm

During an eye examination, ophthalmologist uses retinal (fundus) images to examine the health of an eye. Retinal images are 2-D projection of 3-D retinal semi-transparent tissue (inner surface of eye) on an image plane. It consists of macula and optic disc along with vessels converging at it [4]. Optic disc is basically a bright yellowish and circular region in a healthy retinal image, but in case of pathological conditions, the appearance, shape, and colour of the optic disc might change [5]. Figure 4 shows the complete retinal/fundus image with all psychological features (optic disc, optic cup, macula, and blood vessels).

In case of glaucoma disease, the optic nerve gets gradually damaged, and one of the key factors for this damage is high intraocular pressure (IOP) inside the eye [4]. In a healthy eye, pressure varies from 10 to 21 mm Hg, but for the case of ocular hypertension, this value might go above 21 mm of Hg. While clinical examination ophthalmologists perform various diagnostic tests such as tonometry (measure

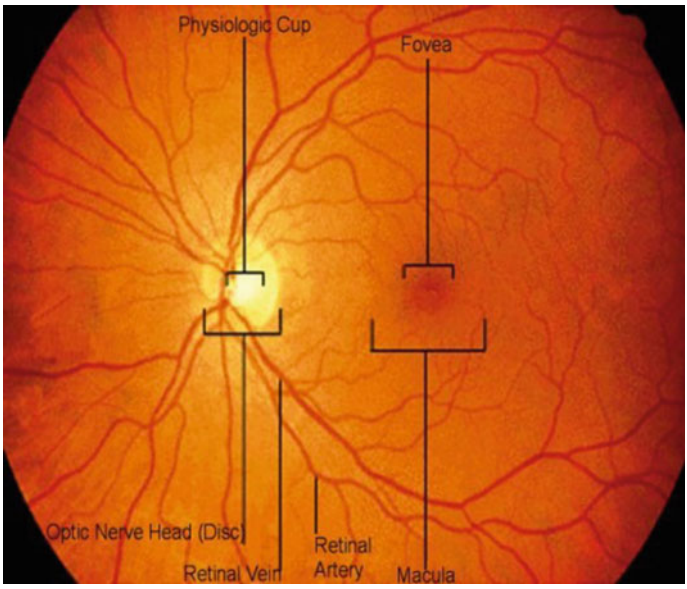

Fig. 4 Normal psychological parts of fundus image

intraocular pressure), pachymetry (determine cornea thickness), gonioscopy (measure drainage angle), disc photography, and visual field test/perimetry (gold standard test) to well diagnose the disease. All these methods require high end technology which is expensive and need well-skilled eye experts to analyse the results. Out of these tests, retinal image analysis is so far the most reliable approach to analyse the disease. The most important indicators for glaucoma are cup-to-disc (CDR) and inferior-superior to nasal-temporal (ISNT) ratios, which can be easily visualized in retinal image photography. The ratio of the diameter of optic cup-to-disc is expressed as a cup-to-disc ratio (CDR). There exists a wide range of C-D ratios for a normal eye [7–9]. In spite of being a strong clinical feature for glaucoma diagnosis, its implementation is really tedious, as finding the cup, and disc boundary is time consuming and requires skilled opticians to annotate the images. Thus, regular/or periodic monitoring of fundus photographs of the optic nerve is required to detect the gradual changes. This point forces one to think to have a device or digital software system which automatically diagnose the eye and give best possible results. Till data researchers have used the traditional approaches of image processing to diagnose the condition of eye. But, with the advent of big data and new technologies, deep learning approaches have become really popular for classification, segmentation, recognition, and various other applications. The deep learning architectures have the ability and flexibility to learn the nested hierarchical features used to represent the world. Its ability to learn generic features like edges, corners etc at bottom level, makes it really interesting to work with. This idea of learning hidden patterns in an image by CNN really motivates us to study and analyse the performance of

various architectures with modified layers. In this paper, an efficient and accurate CNN architecture has been proposed to diagnose glaucoma in retinal images. The selected deep learning network consists of six layers, four consists of convolutional, and last two are fully connected classification layers. The network learns the feature representation of images from large dataset in a supervised end to end fashion.

3 Outline for Deep Learning Convolutional Neural Network

In the fields of self-driving cars, healthcare, finance, robots, and more, the deep learning (DL) has contributed a lot and changed the entire picture in terms of output efficiency. Under the architectures of DL, the convolutional neural networks (CNNs) have been applied broadly to the images and videos for various applications, and one of them is biomedical imaging. The CNN architectures use the nonlinear mapping and spatial scalability to progressively extract the high-level features from the raw input [17]. The hierarchical pattern present in the data is the basic intuition behind the implementation of these networks. For reference, in image processing or computer vision, the lower layers learn the abstract details about the image like edges, blobs, etc., whereas the higher layers recognize the fine and more meaningful details of the input such as alphabets/digits or faces [18].

For the proposed work, we require the CNN architecture as a classification network. In general, the CNN architectures mainly consist of four major components, which are convolutional layer, pooling layer, activation functions, and fully connected layers. We have briefly described each of these as follows.

3.1 Convolutional Layers

These are the basic building blocks in any CNN network, and the raw input image is fed to this layer of network. It simply performs the convolutional operation between the raw image and the designed filter, thus gives a feature map for different filters of varying sizes. The convolutional layer mainly learns the basic patterns present in the image, i.e. edges, blobs and contours, etc.

Mathematically, let $L^{(n-1)}$ and $L^{(n)}$ to be the input and output of nth layer, respectively. Also, it consists of filters of small spatial dimension, which slides over the entire input and gives the feature maps after giving the dot product between filter and image at each location. The filter values are learnable and updated after each new image set. For a CNN network with M layers, L^0 implies the input raw image, and L^M denotes the final output map of nth layer. Finally, we can represent the output of each convolutional layer as a linear mapping of inputs, i.e.

$$L^n = L^{n-1} * w^n + b^n, \tag{1}$$

where w^n, b^n represents the weights and biases for the nth layer. The output dimension of each layer can further be calculated using $(I–F + 2P)/S + 1$, where I is input image size, F is filter size, P is amount of zero padding done, S is stride applied. This layer extracts the deep hierarchical features present in the image, which in general, cannot be seen with naked eye.

3.2 Pooling Layer

A deep CNN networks have millions to billions of trainable parameters. Thus, to reduce the resources required for training such large number of parameters, a pooling layer has been introduced which reduces the spatial dimension of an image by a specified ratio. The most common filter size is 2×2 with stride 2 is applied to reduce the image dimension by half. In general, pooling is categorized into average and maximum pooling, where in the former case, average of four numbers (within 2×2 region) in latter maximum is computed, respectively. In general, pooling layers sum up the statistical features of a feature over the local regions. Apart from all of this, pooling also helps to maintain the translation invariant property in the image. Any local shift/translation at the local pixel level can be made invariant with the pooling operation [36], thus summarizes the output at local neighbourhood.

3.3 Activation Function

CNN tries to learn the nonlinear mapping present in the input image in order to extract the useful hidden features present and solve complex tasks. This function of nonlinearity is performed by the activation functions. It generally follows the convolutional layers in the CNN architectures. As previously mentioned, the convolutional output of each layer by Eq. (1) can be further modified as

$$L^n = f(L^{n-1} * w^n + b^n),$$

where f is the activation function used. In general, the most common activation functions are sigmoid or logistic, tanh and Relu. These functions are used for all convolutional layers except the last final convolutional layer.

3.4 Fully Connected Layer

It is the final fully connected convolutional layers and uses softmax as the activation function. These layers are more specific to the datasets and learn more abstract and detailed information of the data. The various tasks performed by CNN network such as classification, segmentation, localization are decided by the pattern of these layers. These layers represent the feature vectors which hold the aggregated an composite information from all previous convolutional layers.

4 Proposed Deep Architecture for Glaucoma Classification

The proposed convolutional neural network architecture uses four convolutional layers with two fully connected layers, will extract the hierarchical information of images to classify between glaucoma and non-glaucoma images. The details about the network have been explained in the following subsection and the complete architecture has been shown in Fig. 5.

4.1 Region of Interest (ROI) Extraction and Data Augmentation

Unlike the Chen [21] implementation, the network inputs the cropped optic disc as the region of interest of glaucoma detection, and we have used complete retinal image as the region of interest for the problem in hand. The reason is to encounter all possible features present in the complete image, including the key indicators outside the optic disc boundary such as retinal nerve fibre layer (RNFL) defect which suggested to be a strong measure for glaucoma after rim loss.

In the first step of extraction, the image has been cropped such that only field of view (FOV) is present, which avoid the unnecessarily information present in the background and also reduce the noise presence. In the latter step, the images have

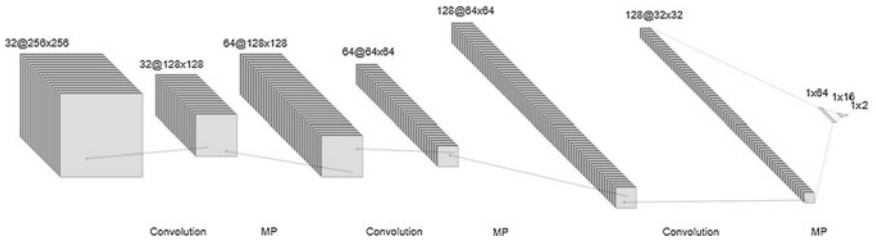

Fig. 5 Proposed architecture

been downscaled to 256 × 256 to reduce the time complexity of algorithm. In deep learning, the models do not generalize well on small datasets, thus suffer from overfitting problem. Although, in practice, the amount of data is limited. Some of the techniques to avoid this are to add normalization term, dropout layers, data augmentation or synthetically generate new images using methods like synthetic minority oversampling technique (SMOTE), generative adversarial networks (GANs) [20], etc. In object recognition problems, data augmentation has been observed as an effective technique [36]. In our proposed work, we employed data augmentation technique to increase the data points/samples, which enhance the variety of data for training. The various transformations used for data augmentation are horizontal flipping, vertical flipping, rotations with an increment of 30° within range of 0° to 360°, horizontal and vertical shifts within 0.2 range, and zooming in/out with 0.3, centre normalization and contrast enhancement. A combination of some of these transformations has also been employed to increase the effective accuracy of the proposed model.

4.2 Layer Architecture and Regularization Methods

The glaucoma classification problem has been modelled as the binary classification problem, where the input is the RGB retinal image and output is a scalar value, predicting the probability of the input image being a glaucomatous image. The architecture consists of four convolution layers with two fully connected layers. The best network has been selected after experimenting with various number of convolutional layers, fully connected neurons count, and different filter sizes. We have used the rectified linear unit (ReLu) activation function for all the convolutional layers except the last. This function is nonlinear in nature and less computationally expensive than "tanh" and "sigmoid" as it involves simpler mathematical operations. Also, it deals with the vanishing gradient problem where in case of low or zero error, the gradient of error is not able to reach the starting layers. For training the network, we have used binary cross entropy loss function to optimize the objective, and ADAM optimizer with learning rate of 0.00001 has been employed to achieve the minima for the cost function. The network has been trained for 200 epochs, with a batch size of 16. The final output layer uses the sigmoid activation for classifying the input retinal images. While training the network, binary cross entropy loss function is computed, and the system parameters (weights) are updated after each epoch. During testing, the image is resized and fed to the trained model for classification. The complete architecture, specifying the size of each filter, along with the dimension has been shown in Table 1.

Table 1 Detailed pipeline for the proposed architecture

Layer name	Output size	Filter size	Kernels	Stride
Conv1	256 × 256	3 × 3	32	1
MAX Pool	128 × 128	2 × 2	32	2
Conv2	128 × 128	3 × 3	32	1
MAX Pool	64 × 64	2 × 2	32	2
Conv3	64 × 64	3 × 3	64	1
MAX Pool	32 × 32	2 × 2	64	2
Conv4	32 × 32	3 × 3	128	1
FCConv1(dense)		–	64	–
FCConv2	–	–	16	–
FCConv2	–	–	2	–

5 Experiments and Simulated Results

The proposed model performance has been verified on Drishti [37], high-resolution fundus (HRF) and Refugee [38] datasets. The former "Drishti dataset has 31 normal and 70 glaucomatous (total of 101) images". All images were taken under a fixed protocol with 30° field of view, centred on the OD and of dimension 2896 × 1944 pixels each image, ground truth was collected from three glaucoma experts, referred to as Expert-1, Expert-2, and Expert-3 with experience of 3, 5, and 20 years, respectively. Next, HRF has 15 glaucomatous and 15 normal images with 3504 × 2336 image dimension, captured using a Canon CR-1 fundus camera with a field of view of 45° and different acquisition setting. At last, the Refugee dataset has 80 glaucoma and 360 non-glaucoma (total of 400) images with 1634 × 1634 image dimension. Thus, for the experimentation, we have 165 glaucoma and 406 normal images. The complete set of databases used for experimentation has been shown in Table 2.

For the assessment of our architecture performance, the data has been divided into 70% training, 10% validation, and 20% testing. Usually, when working with neural networks, evaluating results directly on the testing set can easily result into over-fitting problems, so it is better to first validate the performance on a small set for tuning the parameters and layers. Figures 6 and 7 show the loss and accuracy curve for training and validation datasets for 200 epochs while training the model. It is clearly visible that the train and validation losses decrease with epochs and

Table 2 Detailed glaucoma public datasets

S. No	Dataset name	Glaucomaa	Normal	Dimension
1	Drishti	70	31	2896 × 1944
2	Refugee	80	360	1634 × 1634
3	HRF	15	15	13504 × 2336

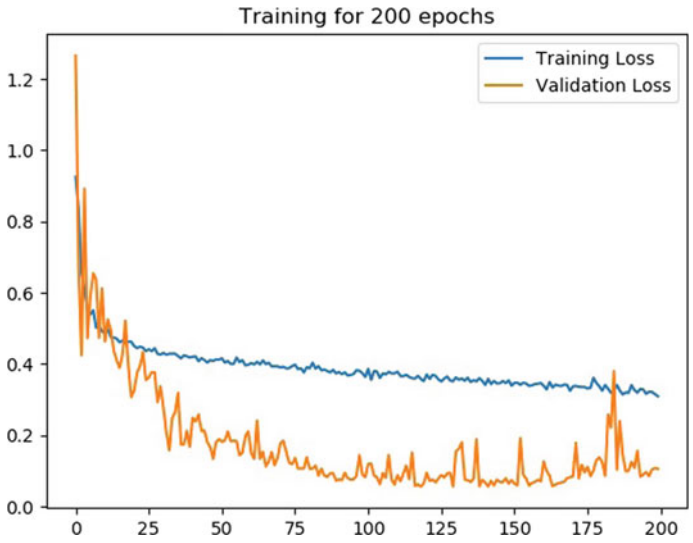

Fig. 6 Loss curve

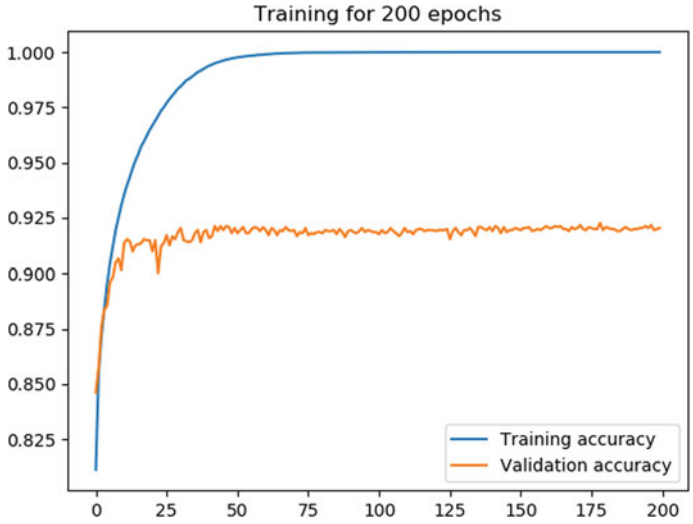

Fig. 7 Accuracy curve

converges near to each other. Although, the model suffers from small over-fitting problem, due to less variance of data, which can easily be dealt with more input data. Also, Table 3 shows the detailed classification results for each dataset individually and collectively. Table 4 shows the complete list of evaluation metrics evaluated for the proposed work.

Table 3 Detailed Results for Classification

Subject samples used for training	samples used for testing	correctly classified samples	% age correct prediction		
Total	Normal	131	25	21	84
	Glaucoma	140	25	24	96
	Total	271	50	45	95.0
Refugee	Normal	100	10	10	100
	Glaucoma	70	10	10	100
Drishti	Normal	21	10	8	80
	Glaucoma	60	10	10	100
HRF	Normal	10	5	3	60
	Glaucoma	10	5	4	80

Table 4 Results of sensitivity, specificity, and positive predictive value classifier

TP	FP	TN	FN	Sensitivity(%)	Specificity(%)	Positive predictive value(%)	Accuracy(%)	F-1 score
24	4	21	1	96	84	85.72	90.0	91.45

5.1 Evaluation Metric

For evaluating our results, we have calculated the accuracy, sensitivity, specificity, and positive predictive rate (PPR) measures for Drishti, HRF, and Refugee datasets. Accuracy is the degree to which the calculated result matches the ground truth (standard). For defining the accuracy mathematically, we have used true positive (TP) and true negative (TN), false positive (FP), false negative (FN) values, where TP represents the images classified as glaucomatous and they are actually glaucomatous, TN is the number of images which are correctly classified as healthy, and actually, they were healthy. False positive (FP) is the healthy images misclassified as glaucomatous, and lastly, false negative (FN) is the glaucomatous samples identified as normal. The other parameters used for evaluation can be easily derived from these definitions. Sensitivity can be defined as glaucomatous category classified as glaucomatous or unhealthy. Specificity can be expressed as probability of normal being predicted as normal class. The positive predictive value (PPV) or precision defines how best one can classify each class. Also, F1-score has been evaluated which measures the test's accuracy. Figure 8 shows some of the results of predicted glaucoma score, first row is the set of glaucoma images, and second row shows the healthy images, respectively.

Thus, accuracy, specificity, sensitivity, and positive predictive value (PPV) can be defined as

$$\text{Accurcay} = \frac{\text{TP} + \text{TN}}{\text{Total no of images}}$$

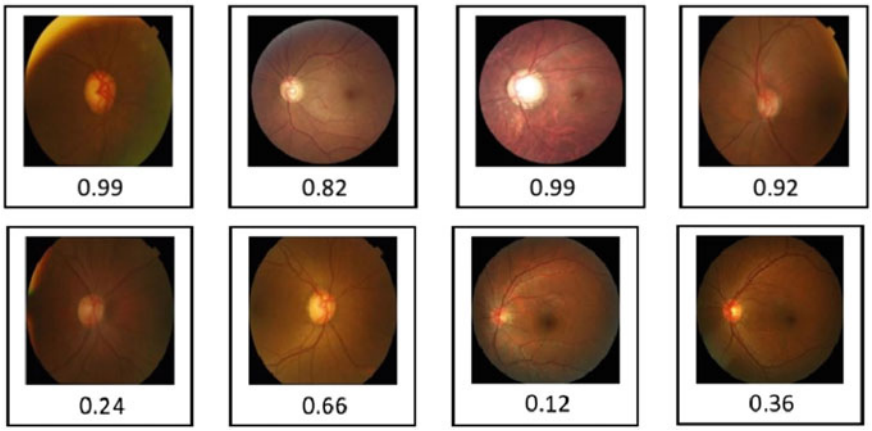

Fig. 8 Predicted glaucoma score for glaucoma and normal images

$$\text{Specificity} = \frac{\text{TN}}{\text{TN} + \text{FP}}$$

$$\text{Sensitivity} = \frac{\text{TP}}{\text{FN} + \text{FP}}$$

$$\text{Positive predictive value (PPV) or Precision} = \frac{\text{TP}}{\text{TP} + \text{FP}}$$

$$F1 - \text{score} = \frac{2 * \text{TP}}{2 * \text{TP} + \text{FP} + \text{FN}}$$

The proposed algorithm has been implemented using Keras library and NVIDIA Quadro P5000 GPU, with 128 GB RAM on windows 10 system.

6 Conclusion

Globally, the glaucoma is an irreversible eye disease that retinal disease that affects several people globally every year. Glaucoma is a chronic eye disease in which the optic nerve gets gradually damaged and thus leads to permanent loss of vision. Globally, it affects several people and thus becomes the second leading cause of eye diseases. Most of the conventional image processing techniques for glaucoma diagnosis require laborious manual inputs from a skilled eye specialist, i.e. ophthalmologists in terms of building the ground truths for the optic disc and cup boundaries. Hence, it is necessary to develop a robust and more efficient methods for glaucoma detection. Automation provides a more viable and effective solution to this problem of glaucoma detection. A proposed algorithm classifies the retinal fundus images using automated approach based on deep convolutional neural network architecture. This algorithm consists of four convolutional layers with two fully connected layers

to attain accuracy of 90.0% and F-1 score of 91.45% on image classification, respectively. The proposed network has faced a over-fitting problem even after applying augmentation and dropouts. The reason is limited amount of data for the training, and thus, our future work is to collect large data to enhance the robustness of the algorithm. Apart from this, our algorithm follows a general classification problem and can be used for other medical image classification problems.

References

1. World Health Organization Media centre: visual impairment and blindness
2. Rogers K (2011) The eye: the physiology of human perception, First edn. Britannica Educational Publishing, 29 East 21st Street, New York, NY
3. Glaucoma Foundation (2012) Understanding and living with glaucoma, pp 1–36, 2012
4. Bhowmik D, Kumar KS, Deb L, Paswan S, Dutta AS (2012) Glaucoma—a eye disorder. Its causes, risk factors, prevention and medication. Pharma Innov 1(1):66–82, 2012. Retrived from www.Thepharmajournal.Com
5. Narasimhan K, Vijayarekha K (2011) An efficient automated system for glaucoma detection using fundus image. J Theor App Technol 33(1):104–110
6. Sharangouda N (2015) Automated glaucoma detection in retina from cup to disk ratio using morphology and vessel bend techniques. Int J Adv Res Comput Commun Eng 4(6):139–142
7. Anderson D (2013) The optic nerve in glaucoma. Duane's Ophthalmol., p. chap 48
8. Sivaswamy J et al (2015) A comprehensive retinal image dataset for the assessment of glaucoma from the optic nerve head analysis. JSM Biomed Imaging Data Papers 2(1)
9. Sri Abirami S et al (2013) Glaucoma images classification using fuzzy min-max neural network based on dta-core. Int J Sci Mod Eng (IJISME) 1(7). ISSN: 2319–6386
10. McIntyre R et al (2004) Toward glaucoma classification with moment methods. In: Proceedings of the first Canadian conference on computer and robot vision. IEEE
11. Almazroa A, Alodhayb S, Raahemifar K, Lakshminarayanan V (2017) An automatic image processing system for glaucoma screening. Int J Biomed Imaging vol 2017, Article ID 4826385, 19 pages
12. Almazroa A, Alodhayb S, Osman E, Ramadan E, Hummadi M, Dlaim M, Alkatee M, Raahemifar K, Lakshminarayanan V (2018) Retinal fundus images for glaucoma analysis: the RIGA dataset. In: Medical imaging 2018: imaging informatics for healthcare, research, and applications, pp 8
13. Sun W, Alodhayb S, Almazroa A, Raahemifar K, Lakshminarayanan V (2017) Optic disc segmentation for glaucoma screening system using fundus images. Clin Ophthalmol 11:2017–2029
14. Kumar BN, Chauhan RP, Dahiya N (2016) Detection of glaucoma using image processing techniques: a review. In: 2016 international conference on microelectronics, computing and communications (MicroCom). Durgapur, pp 1–6. https://doi.org/10.1109/micro-Com.2016.7522515
15. Acharya UR, Du Dua S, Du X, Sree V, Chua CK (2011) Automated diagnosis of glaucoma using texture and higher order spectra features. Inform Technol Biomed IEEE Trans 15(3):449–455
16. Society. 27th Annual International Conference of the, pp 6608–6611 IEEE, 2006
17. Krizhevsky A, Sutskever I, Hinton GE (2017) ImageNet classification with deep convolutional neural networks. Commun. ACM 60(6):84–90. https://doi.org/10.1145/3065386
18. Simonyan K, Zisserman A (2015) Very deep convolutional networks for large-scale image recognition. In: ICLR
19. Goodfellow I, Bengio Y, Courville A (2016) Deep learning. MIT Press
20. Goodfellow IJ, Pouget-Abadie J et al (2014) Generative adversarial networks. arXiv:1406.2661

21. Chen X, Xu Y, Wong DWK, Wong TY, Liu J (2015) Glaucoma detection based on deep convolutional neural network. In: 2015 37th annual international conference of the IEEE engineering in medicine and biology society (EMBC). Milan, pp 715–718. https://doi.org/10.1109/embc.2015.7318462
22. Abramoff M (2010) Retinal image analysis. Eng IEEE Rev 169–208
23. Wong DK et al (2008) Level-set based automatic cup-to-disc ratio determination using retinal fundus images in ARGALI. In: Conference in proceedings of IEEE engineering in medicine and biology society, vol 2008, no 2, pp 2266–2269
24. Liu J et al (2009) ARGALI: an automatic cup-to-disc ratio measurement system for glaucoma analysis using level-set image processing. In: Lim CT, Goh JCH (eds) 13th international conference on biomedical engineering. IFMBE proceedings, vol 23. Springer, Berlin, Heidelberg
25. Cheng J et al (2013) Superpixel classification based optic disc and optic cup segmentation for glaucoma screening. IEEE Trans Med Imaging 32(6):1019–1032. https://doi.org/10.1109/TMI.2013.2247770
26. Yin F et al (2012) Automated segmentation of optic disc and optic cup in fundus images for glaucoma diagnosis. In: Proceedings of IEEE symposium on computer-based medical *systems*
27. Juneja M, Singh S, Agarwal N et al (2019) Automated detection of Glaucoma using deep learning convolution network (G-net). I:n Multimed Tools Appl. https://doi.org/10.1007/s11042-019-7460-4
28. Xu Y et al (2011) Sliding window and regression based cup detection in digital fundus images for glaucoma diagnosis. In: Fichtinger G, Martel A, Peters T (eds) Medical image computing and computer-assisted intervention—MICCAI 2011. MICCAI 2011. Lecture Notes in Computer Science, vol 6893. Springer, Berlin, Heidelberg
29. Xu Y, Lin S, Wong DWK, Liu J, Xu D (2013) Efficient reconstruction-based optic cup localization for glaucoma screening. In: Mori K, Sakuma I, Sato Y, Barillot C, Navab N. (eds) Medical image computing and computer-assisted intervention—MICCAI 2013. MIC-CAI 2013. Lecture Notes in Computer Science, vol 8151. Springer, Berlin, Heidelberg
30. Sevastopolsky A (2017) Pattern recognit. Image Anal 27:618. https://doi.org/10.1134/S1054661817030269
31. Mvoulana A et al (2017) Fully automated method for glaucoma screening using robust optic nerve head detection and unsupervised segmentation based cup-to-disc ratio computation in retinal fundus images. Comput Med Imaging Graph 101643. https://doi.org/10.1016/j.compmedimag.2019.101643. Epub 2019 Aug 14
32. Al-Bander B, Williams BM, Al-Nuaimy W, Al-Taee MA, Pratt H, Zheng Y (2018) Dense fully convolutional segmentation of the optic disc and cup in colour fundus for glaucoma diagnosis. Symmetry 10:87
33. Diaz-Pinto A et al (2019) CNNs for automatic glaucoma assessment using fundus images: an extensive validation. J BioMed Eng OnLine. https://doi.org/10.1186/s12938-019-0649-y
34. Chen X, Xu Y, Yan S, Wong DWK, Wong TY, Liu J (2015) Automatic feature learning for glaucoma detection based on deep learning. In: Navab N, Hornegger J, Wells W, Frangi A (eds) Medical image computing an computer-assisted intervention—MICCAI 2015. MICCAI 2015. Lecture Notes in Computer Science, vol 9351. Springer, Cham
35. Abbas Q (2017) Glaucoma-deep: detection of glaucoma eye disease on retinal fundus images using deep learning. Int J Adv Comput Sci Appl (IJACSA) 8(6). http://dx.doi.org/10.14569/IJACSA.2017.080606
36. Bengio Y, Courville A, Goodfellow IJ (2016) Deep learning adaptive computation and machine learning. The MIT Press
37. Sivaswamy J, Krishnadas SR, Joshi GD, Jain M, Tabish AUS (2014) Drishti-GS: retinal image dataset for optic nerve head(ONH) segmentation. In: 2014 IEEE 11th international symposium on biomedical imaging (ISBI). Beijing, pp 53–56
38. Xu Y Chinese Academy of Sciences, China, https://refuge.grand-challenge.org/